A simple model of a water column applied to the deep water formation in Northern Catalan Sea

J. L. LÓPEZ-JURADO ([1]), J. TINTORÉ ([2,3]), J. SALAT ([3]),
LI. MIRALLES ([3]), A. JANSÀ ([4])

([1]) *Instituto Español de Oceanografía, Palma de Mallorca.*
([2]) *Facultat de Ciències Físiques, Universitat de Palma de Mallorca.*
([3]) *Institut de Ciències del Mar, Barcelona.*
([4]) *Centro Meteorológico Zonal, Palma de Mallorca.*

ABSTRACT. In this paper an attempt to reproduce the evolution of the thermal structure of water columns by a simple one-dimensional model is presented. The model is based on the heat balance between the sea and the atmosphere and it is especially sensitive to air temperature and wind speed.
The model is used to study the influence of these atmospheric forcings on the deep water formation process in the Northern Catalan Sea. It is applied using meteorological and oceanographic data collected during the ALPEX Special Observation Period (SOP) and the results are compared to temperature profiles obtained during the CARON 82 cruise (MEDALPEX).

Key words: Northwestern Mediterranean, deep water formation, water column model, ocean-atmosphere heat balance, thermal vertical structure, MEDALPEX.

Annales Geophysicae, 1987, **5B,** (1), 55-60.

INTRODUCTION

The formation of deep water in the Gulf of Lions and in the Northern Catalan Sea is one of the essential features of the oceanography of the Western Mediterranean. This process, studied by both oceanographers and meteorologists during the last 15 years (MEDOC Group, 1970), represents one of the most interesting examples of air-sea interaction on small space and time scales.

The area of deep water formation is approximately centered at the point 42° N 5° E, South of the Gulf of Lions. The cyclonic circulation of the basin induces a surface divergence, a permanent doming of isopycnals and therefore the presence of dense waters in the central part of the region (Font *et al.*, 1986). These features play an essential role in the process of destabilization of the water column during winter.

The strong, dry and cold, continental winds (Mistral and Tramuntana) cool the oceanic surface layer and increase its salinity, thereby increasing its density. The instability of the water column gives rise, in some regions, to episodes of very intense convective motions which can reach the deepest levels. According to Gascard (1978), during these wind episodes, very strong downwards velocities have been recorded, up to 10 cm s^{-1}, within convective cells whose horizontal scale is about 10 km, similar to the internal Rossby radius of deformation in the area.

The formation of these small scale regions of deep convection is still not completely understood. Gascard (1978) proposed an explanation in terms of oceanic eddies and he found a good agreement between the results from a baroclinic instability model (Tang, 1975) and the observations from the MEDOC 75 cruise. Crépon *et al.* (1982) showed the existence of large amplitude baroclinic waves in the Ligurian Sea and they found also good agreement between the wavelengths and phase velocities observed and those predicted by the model of Tang (1975).

The CARON Project (1982-83), a Spanish contribution to MEDALPEX, was designed to obtain some more information on the mechanisms of deep water formation and to determine its horizontal extent to the South, since previous cruises in the Catalan Sea had shown intense convective motions in this region, South of the Gulf of Lions. The objective of this paper is to use some of the results from the CARON cruises to simulate the different convection processes observed, by means of a simple one-dimensional model of the thermal structure of the water column.

MATERIAL AND METHODS

The CARON cruises

The CARON 82 cruise, from 6 to 11 March 1982, during the ALPEX Special Observation Period (SOP) took place immediately after the strongest Mistral episode observed during the SOP, on March 5. During

this cruise, 18 stations with a high resolution CTD (Neil Brown) and continuous analysis of surface temperature and salinity, along the path of the ship, were performed (fig. 1). In 1983, from February 23 to March 11, another cruise, CARON 83, in the same region was carried out using the same methodology.

Description of the model

A simple one-dimensional discrete model, based on the energy transfer (heat budget and turbulent diffusion) in the water column, is constructed and used to study the evolution of the thermal structure. The water column is divided into discrete layers. Every layer, n, is supposed to be homogeneous in temperature and with characteristic thickness, Δz_n and extinction coefficient, k_n. From an initial temperature profile, the model gives the daily evolution of this profile on the basis of meteorological data. The work of the model can be described in two steps :

In the first step, the heat budget is evaluated for every day. In the second step, the result from the previous step is used to modify the initial thermal structure : if the result from the heat budget is positive, absorption of solar energy will take place, while convective mixing occurs if the budget is negative. In both cases, a redistribution will take place due to turbulent diffusion.

The limitation of the model are essentially due to the fact that surface waves, horizontal advection and salinity effects are not included. Salinity is assumed to be constant throughout the water column and therefore evaporation effects are not properly included.

First step

The heat budget is calculated using two terms. The first term is the radiation term (radiation that enters the surface layer) and the second term accounts for all the losses due to evaporation, sensible heat flux and long wave radiation. The difference between those two terms establishes the gains and losses of the water column.

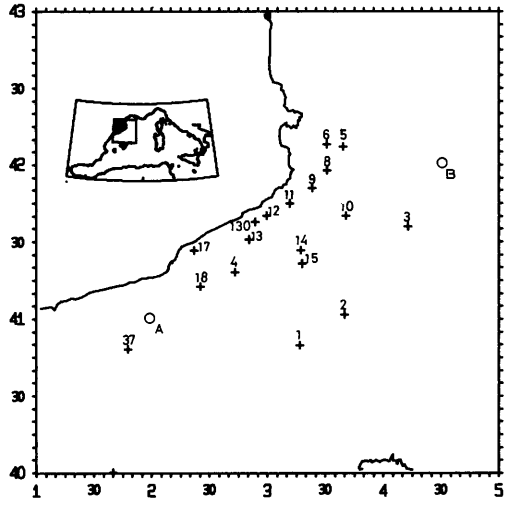

Figure 1
Positions of the stations of the cruise CARON 82 *and the points* A *and* B *selected for simulation.*

The radiation term (solar irradiance that penetrates the sea surface) is evaluated from the observed data.

The losses of energy are evaluated as follows :

— net terrestrial irradiance :

$$Q_b = 0.985\,\sigma T^4\left(0.39 - 5.04\,10^{-2}\,\left(rE_s\right)^{1/2}\right)\,,$$

where σ is the Stefan-Boltzmann constant, T is the absolute temperature, $r = E_a/E_s$, being E_a the water vapour pressure at the air temperature and E_s the saturated water vapour pressure at the sea surface temperature. This expression is used affected by a cloud correction factor $\left(1 - 0.6\,C^2\right)$, where C is the cloud coverage in tenths.

— evaporation :

It is calculated by a Dalton type formula proposed by Laevastu (1976) :

$$Q_e = 5.26\,10^{-3}\,vE_s\,(1 - r)\,,$$

where v is the wind speed in m s^{-1};

— sensible heat flux :

This flux is evaluated using the Bowen ratio, R_b, approach :

$$Q_i = R_b\,Q_e\,,$$

where

$$R_b = 0.64\left[\left(T_s - T_a\right)/\left(E_s - E_a\right)\right].$$

A sensitivity analysis of the losses of energy was made to study the relative importance of the different variables. The global heat budget is found to be especially sensitive to the wind speed and sea surface temperature (fig. 2).

Second step

— absorption of solar irradiance at sea :

When the result of the heat budget is positive, we assume that the energy input is distributed in the water column. The amount of energy absorbed in the layer n is deduced by evaluating the irradiance, I_n, at the depth, from the irradiance received in the former layer, I_{n-1}, and the extinction coefficient, k_n, for this layer, according to

$$I_n = I_{n-1}\exp\left(-k_n\,\Delta z_n\right)\,,$$

where Δz_n is the thickness of the layer.

Once the absorption in each layer is known, we estimate the temperature increase, ΔT, and the original temperature distribution is modified accordingly ;

— convective motions :

Whenever the global heat budget is negative, which is the most common situation during this application, we can assume that these losses are only due to surface cooling, then we compute the temperature difference ΔT corresponding to these losses in the upper layer. The density will therefore increase and this will lead to an unstable stratification in the upper layer. The

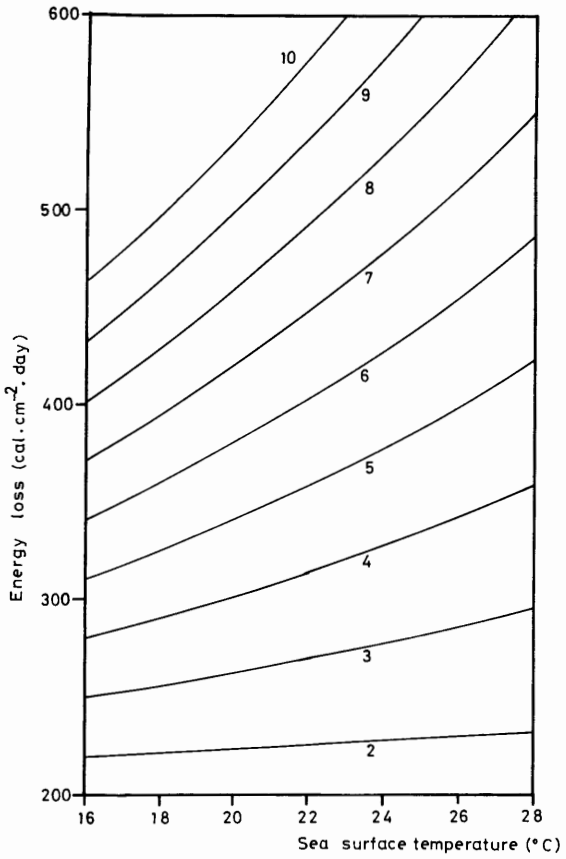

Figure 2
Sensitivity analysis : total energy loss versus *sea surface temperature at a constant wind speed* (m s^{-1}).

net result will be the formation of a convective mixing down to a depth where the resulting density of the mixing will be equal to that of the surrounding waters ;

— turbulent diffusion :

As already mentioned, once the absorption or convective mixing processes have taken place, the model simulates the process of redistribution by vertical turbulent diffusion computed through the vertical turbulent flux

$$F_z = - C\rho K_z \Delta T/z ,$$

where ρ is the mean density in the water column, C the specific heat and K_z the turbulent diffusion coefficient.

Since the model deals with individual layers, the temperature difference ΔT in each layer due to vertical turbulent fluxes will be given by the difference between heat entering and leaving the layer. In this way we obtain the redistribution of energy in the water column.

Model data

The extinction and diffusion coefficients used in this paper are taken from Sverdrup *et al.* (1942) for oceanic water and weak stability.

Meteorological data required (dry bulb temperature, wind speed, dew point temperature) for the model have been taken from an objective analysis (Jansà *et al.*, 1986). Geostrophic winds, corrected for friction by subtracting 1/3 of their magnitude, have been used. Winds are, therefore, underestimated for the Gulf of Lions area so that the simulated effects are expected to be lower than the observed ones.

Irradiance values have been taken from INM (1984) from Tarragona and Maó for the coastal and offshore stations respectively. Cloud coverage data used came from Barcelona and Maó.

RESULTS

The CARON observations

The geostrophic wind pattern clearly shows northerlies (fig. 3), which are necessary for the deep water formation process to take place. The data obtained show some evidence of cells of deep water formation, usually known as *chimneys*, and the zone, where deep water formation occurs, appears bounded by lateral fronts (Font *et al.*, 1986).

Summarizing the results, three distinct zones can be identified (fig. 4) :

— a zone of continental influence characterized by the presence of cooler and fresher waters at the surface, submitted to strong winds,

— a deep water formation zone with high values of salinity in the surface layer, also under the influence of strong winds, and

— a zone of stratified waters, showing some remainder of thermocline, over which warmer and more humid winds blow.

The information obtained during the CARON 83 cruise confirmed some of the hypotheses and facts established during CARON 82, in particular those which refer to the extent of the deep water formation zone, the presence of a front along the eastern boundary and the structure of the chimneys (Salat and Font, 1987).

Numerical results

The model has been run for two stations (fig. 1) : A, lying in the zone under continental influence, and B, in the deep water formation area. In both cases we assume that the water column is initially isothermal at a temperature of 13 °C, characteristic of this area. The model has also been run in a third case, using the oceanographic data from stations 4 and 18 (CARON 82), and the meteorological data from the time period between the two stations. The temperature distributions obtained from the model for the three cases are represented in figures 5, 6 and 7.

DISCUSSION

The model allows us to distinguish clearly atmospheric situations leading to the onset of stable or unstable stratification in the water column. The results of the different heat budgets allow to different

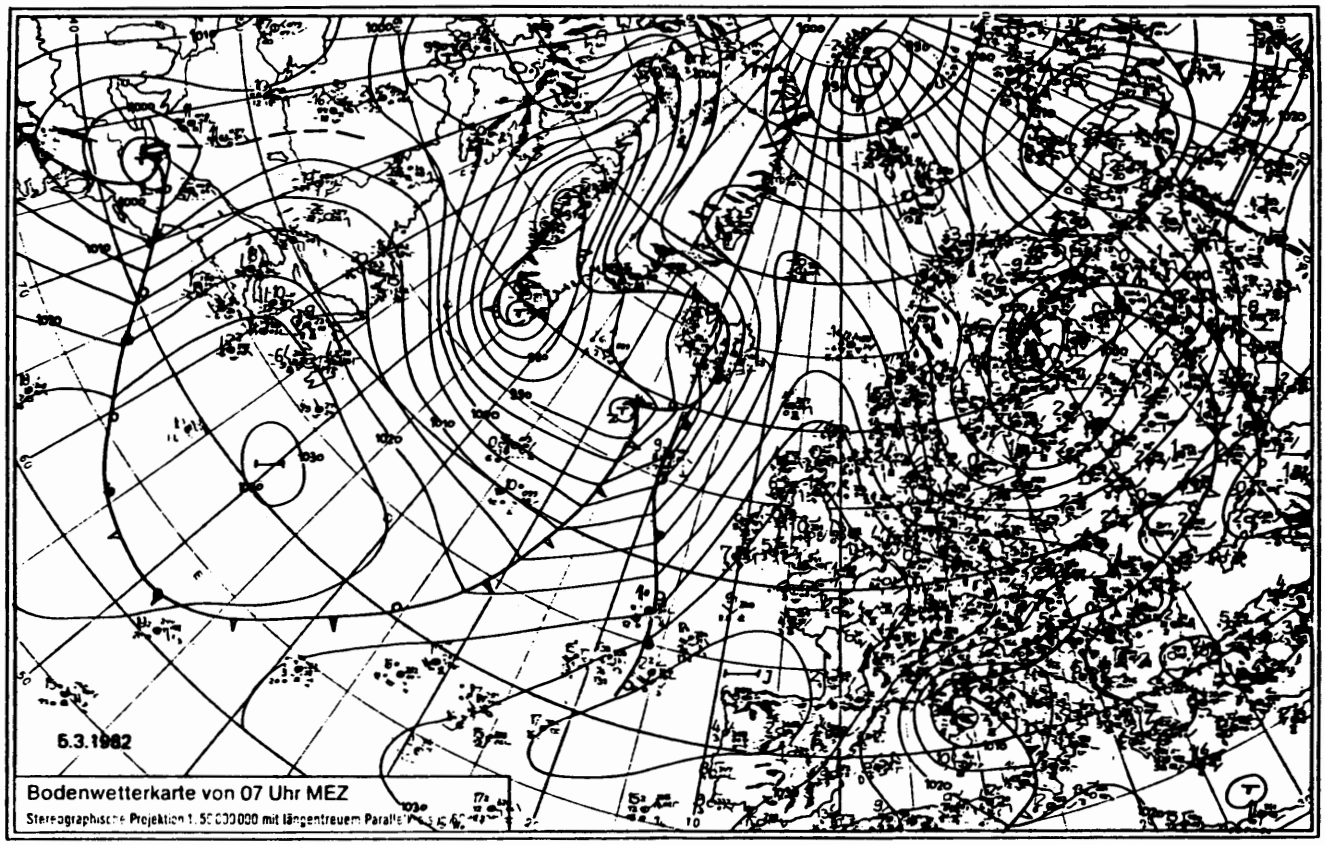

Figure 3
Surface weather chart for 5 March 1982 (0600 GMT). *Extracted from :* GARP-ALPEX No. 6A.

situations : negative budgets, being associated with surface cooling, are followed by vertical motions, and positive budgets by surface heating and stratification. The values of the different components of the budget for the 3 cases studied (table 1) agree with the expected behaviour. The value of net irradiance from the ocean, Q_b, remains close to a mean value of 161 cal cm^{-2} day^{-1}, which is slightly larger than the mean values given by Colacino and dell'Osso (1977).

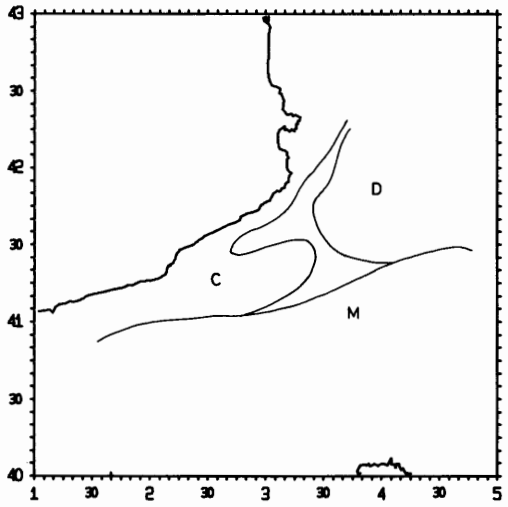

Figure 4
Surface water mass distribution found during CARON 82. D : *deep water,* C : *water under continental influence,* M : *warm and stratified waters.*

The values of solar radiation penetrating in the sea never exceed 380 cal cm^{-2} day^{-1}. Therefore, the successive budgets will be negative and will induce convective motions.

The evolution of the temperature distribution at the point A (fig. 5), shows that the progressive cooling

Table 1

Values of the components of the heat budget for the three cases studied.
Q_b : *net terrestrial irradiance*
Q_i : *sensible heat flux*
Q_e : *evaporation*
Q_t : *total loss of energy*
R : *radiation term*
I_0 : *total heat budget.*

	3/3/82	4/3/82	5/3/82	6/3/82	7/3/82
point A :					
Q_b	151	136	193	193	
Q_i	84	− 39	98	− 27	
Q_e	163	433	579	297	
Q_t	398	530	870	463	
R	303	304	355	364	
I_0	− 95	− 226	− 515	− 99	
point B :					
Q_b	168	120	161	187	
Q_i	− 58	1	408	168	
Q_e	192	266	733	706	
Q_t	302	387	1302	1061	
R	377	353	319	363	
I_0	71	− 34	− 983	− 698	
stations 4 to 18 :					
Q_b	135	171	171	128	177
Q_i	35	78	37	50	− 4
Q_e	68	177	112	152	206
Q_t	238	426	320	330	379
R	271	331	312	292	359
I_0	33	− 95	− 8	− 38	− 20

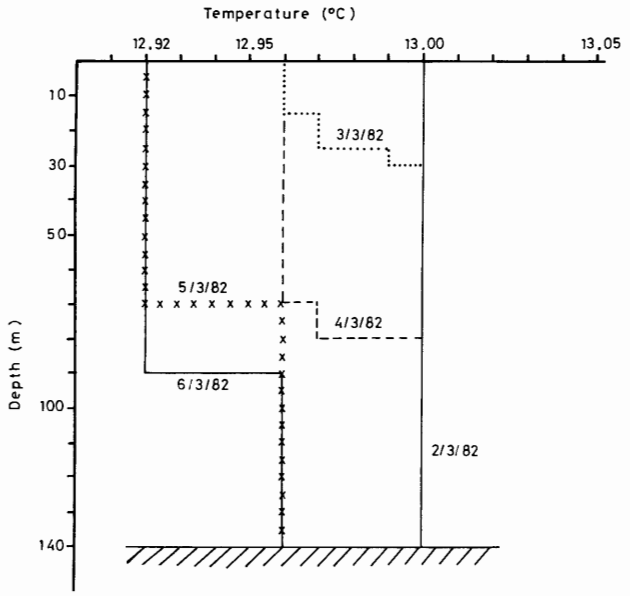

Figure 5
Evolution of the temperature profile at the point A, *simulated by the model.*

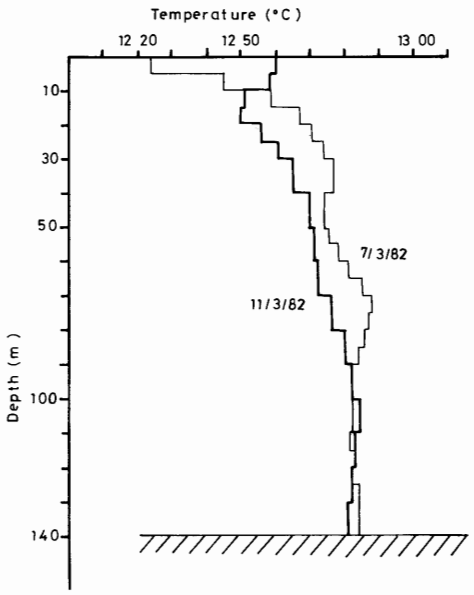

Figure 7
Evolution of the temperature profile from station 18 *to station* 4 (CARON 82), *simulated by the model.*

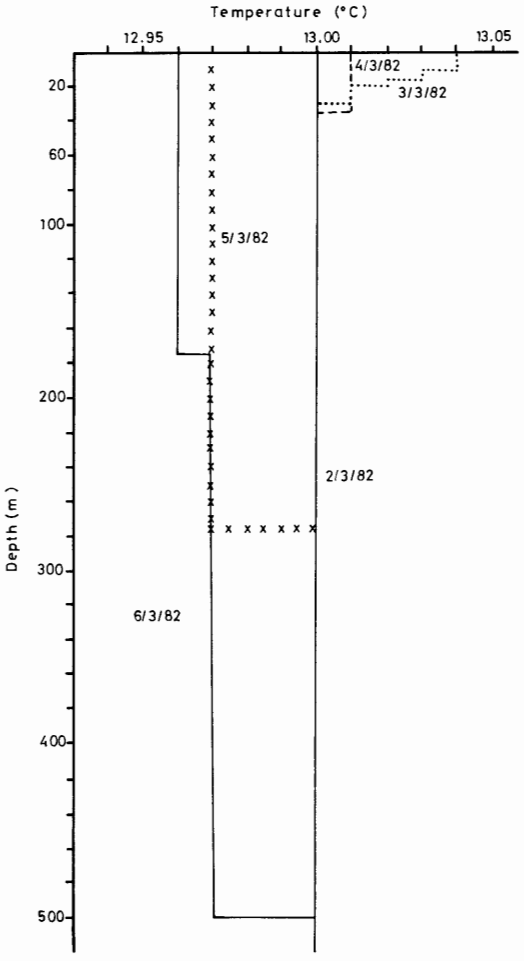

Figure 6
Evolution of the temperature profile at the point B, *simulated by the model.*

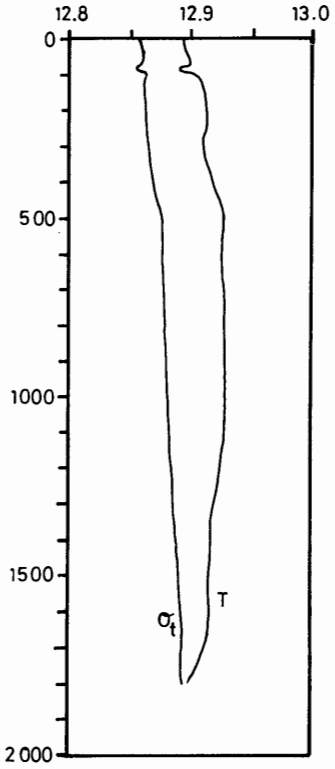

Figure 8
Temperature profile at station 3 (CARON 82).

gives rise to a vertical mixing which tends to homogenize the water column down to increasing depths. The wind episode of March 5 was especially significant, since the largest negative budget was recorded on that day (515 cal cm^{-2} day^{-1}). This cooling strongly affected the whole water column thereby creating a quasi-homogeneous layer of 90 m depth.

Similarly, figure 6 shows the evolution at point B down to a depth of 500 m. Assuming again an initially homogeneous temperature distribution, we observe a slight surface heating corresponding to the positive budget of March 3, followed by an instability due to progressive cooling which gives rise to convection. The surface cooling on March 5 (– 983 cal cm^{-2}

day^{-1}, the largest in the three cases) homogenizes the water column down to a depth of 275 m, while the heat deficit of March 6, although somewhat smaller ($698\ cal\ cm^{-2}\ day^{-1}$) affects the profile down to 500 m.

The evolution of the water column between March 7 (station 18) and March 11 (station 4) (fig. 7) shows that from the initial unstable stratification, convective motions are correctly simulated by the model. The temperature of the upper layers increases until the water column is completely homogeneous.

The analysis of these 3 cases shows that the model correctly simulates the physical processes : initial instability due to surface cooling followed by convection and mixed layer deepening. In the real process, different water masses are involved but this is not taken into account by the model, since neither horizontal advection nor changes in salinity are included. Therefore the models seem especially suitable to simulate the mixed layer formation from a unique water mass. However, the real process is stronger than the simulated one since, in the last, surface evaporation only affects temperature.

The comparison between the results at points A and B shows, as expected, different behaviours due to the different geographical situations. At point A, the cooling is higher in the whole water column while at point B, the cooling is smaller since the volume affected is bigger.

The coincidence between the model's results at point B and the temperature distribution obtained at station 3 (CARON 82) is remarkable. As it is shown in figure 8, the water column is homogeneous down to 1500 m and the difference between surface and bottom temperature is only of 0.04 °C.

In the last case, figure 7, the model output shows the formation of a stable surface layer, and therefore, convective motions will be suppressed until the next negative budget occurs. The model behaviour in this case is too fast, due to the absence of salinity gradients, but it still reflects the real process of stable stratification formation.

The results of this application evidence that salinity plays an important role in the mixing process so that the absence of this variable poses one of the main limitations of this model. Other limitations, like its discrete layered vertical structure, the use of daily averaged input data, or its dependence on parameters whose estimation offers some problems, can be easily counter-balanced by its simplicity.

REFERENCES

Colacino M., Dell'Osso L., 1977. Monthly mean evaporation over the Mediterranean Sea. *Arch. Meteorol. Geophys. Biokl.*, A, **26,** 283-293.

Crépon M., Wald L., Monget J. M., 1982. Low-frequency waves in the Ligurian Sea during december 1977. *J. Geophys. Res.*, **87,** (C1), 595-600.

Font J., Salat J., Tintoré J., 1986. Permanent features in the circulation of the Catalan Sea. *Oceanol. Acta* (in press).

Gascard J.-C., 1978. Mediterranean deep water formation, baroclinic instability and oceanic eddies. *Oceanol. Acta*, **1,** 3, 315-330.

INM, 1984. Radiación solar en España. Centro de Estudios Meteorológicos. Publ. D44. Madrid.

Jansà A., Alonso S., Ramis C., Heredia M. A., García-Moya J. A., 1986. Non-Alpine contribution to Mediterranean cyclogenesis, synoptic study of two cases occurring during ALPEX S.O.P. WMO/TD 108, GARP Publ. series n° 27, Scientific Results of the Alpine Experiment (ALPEX), **2,** 297-308.

Laevastu T., 1976. Oceanic water balance. *WMO series*, **442,** 112 pp.

MEDOC Group, 1970. Observation of formation of deep water in the Mediterranean Sea, 1969. *Nature*, **227,** 1031-1041.

Salat J., Font J., 1987. Water mass structure near and offshore the Catalan coast during the winters of 1982 and 1983. *Ann. Geophysicae*, **5B,** (1), 49-54.

Sverdrup H. U., Johnson M. W., Fleming R. H., 1942. The Oceans. Their physics, chemistry and general biology. Prentice-Hall, Englewood Cliffs NJ, 1087 pp.

Tang C. M., 1975. Baroclinic instability of stratified shear flows in ocean and atmosphere. *J. Geophys. Res.*, **80,** 9, 1168-1175.